

RESEARCH PAPER

Computational study of optical properties, and enantioselective synthesis of di-substituted esters of hydantoic and thiohydantoic acids

Hiwa Omer Ahmad*

*Department of Pharmaceutical Chemistry, College of Pharmacy, Hawler Medical University. Hawler, Kurdistan Region, Iraq.

ABSTRACT:

The title compounds with different optically active substituted ester of hydantoic and thiohydantoic were synthesized by the reaction of corresponding enantio-pure amino acids methyl ester hydrochloride with phenylisocyanate/thiocyanate in the presence of triethylamine. The duration of reaction was limited to avoid racemisation and produce high enantio-enriched compounds. Low values of ELUMO-HOMO gap 0.14, 0.16, 0.15, 0.15, and 0.10 eV were observed for compounds 1, 2, 3, 4, and 5, respectively indicate soft, and high reactivity compounds. Values of ELUMO-HOMO gap also show that the compounds can easily decompose spontaneously to their elements. The order of synthesized compounds based on increasing reactivity depends on LUMO-HOMO energy gap represent as follows; 5>1>3, 4>2. Thermodynamic energies have been calculated for synthesized compounds including Enthalpy and Gibbs free energy.

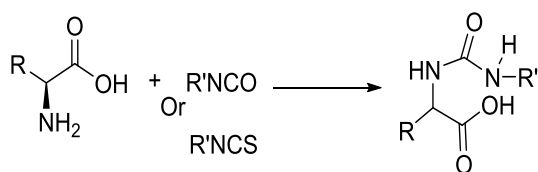
KEY WORDS: Density functional theory calculations; Energy, Molecular electrostatic potential, hydantoic acids.

DOI: <http://dx.doi.org/10.21271/ZJPAS.32.1.9>

ZJPAS (2020) , 32(1);75-94 .

1.INTRODUCTION :

The reaction of α -amino acids with isocyanate or isothiocyanate generally takes place in basic aqueous solution to produce ureido acids. (Scheme 1.1). (Ware, 1950)



Scheme 1.1: The condensation of amino acids with isocyanate or isothiocyanate.

If a large excess of base is used, racemization and/or formation of hydantoin or thiohydantoin (Ballard *et al.*, 2018) take place without formation of optically active hydantoic and thiohydantoic acid. Previously reported that ester of isocyanate reacts with an amine to produce ester of hydantoic acid. (Lombardino and Gerber, 1964)

Computational methods provide accurate, easy and time saving techniques for drug design. (Abdallah, 2019) Orbital energies calculation has been used to obtain ionization potential (*IP*) and electron affinity (*EA*) values for neutral molecules. The negative values of the highest occupied molecular orbital energy ($-E_{\text{HOMO}}$) and the lowest unoccupied molecular orbital energy ($-E_{\text{LUMO}}$) gives information to ionization potential and electron affinity,

* Corresponding Author:

Mukhlis Hamad Aali

E-mail: Hiwa.omar@hmu.edu.krd

Article History:

Received: 14/09/2019

Accepted: 14/10/2019

Published: 25/02 /2020

respectively (i.e., $IP = -E_{HOMO}$ and $EA = -E_{LUMO}$). (Shankar *et al.*, 2009)

The energy level of $E_{LUMO-HOMO}$ for all synthesized compounds elucidate physical and chemical information such as ionization potential (IP), electron affinity (EA), electronegativity (χ), electrophilicity index (ω), hardness (η), softness (S) and chemical potential (μ).

2. Experimental section

2.1 Materials and methods

All starting compounds were obtained from Fisher Scientific, Sigma-Aldrich, Alfa Aesar, Fluorochem, Acros Organic, BDH, and Lancaster Synthesis and used without any further purification. 1H -NMR and ^{13}C -NMR spectra were recorded on Brukeravance (400 MHz) spectrometer. Parts per million is a unit of chemical shift and tetra-methylsilane expressed as a standard. NMR spectra were recorded in solutions in the deuterated solvent mentioned in method section.

Optical rotations were measured with a Schmidt-Haensch Polartronic 1 in a 5.00 cm path length cell. The solvent and concentration (expressed in g/100 ml) of the solutions LCMS experiments were performed using a Waters 2790 liquid chromatography system and a Waters ZQ mass spectrometer. Samples were loaded using a Gilson 232XL auto-sampler. Low-resolution mass spectrometric data were determined using a Fisons VG Platform II quadrupole instrument using electrospray ionisation (ES), unless otherwise stated. High-resolution mass spectrometric data were obtained in electrospray (ES) mode unless otherwise reported, on a Waters Q-TOF micro-mass spectrometer.

2.2 Molecular Modeling

Gaussian 09W was used to perform ab initio molecular orbital (MO) calculations. (Frisch *et al.*, 2016) employing the B3LYP functional and the 6–31 G basis set for all atoms. (Becke, 1993) For molecular structures optimization, GaussView 5.0.9 program was used for HOMO and LUMO surfaces area and electron distribution. (Frisch *et al.*, 2000)

2.3 Energy Minimization Procedure

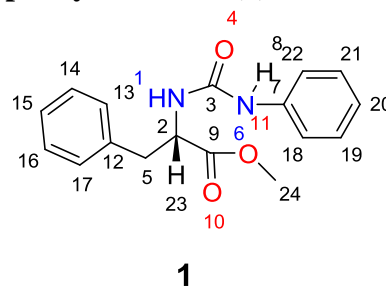
The chemical compounds with the correct stereochemistry were drawn on Chemdraw professional 16.0 and stored in mol format in Gaussian view 5.0.9.

2.4 Chemistry

2.4.1. General procedure

Corresponding amino acids methyl ester hydrochlorides were dissolved in dichloromethane in a round bottom flask in the presence of triethylamine. Phenyl isocyanate/isothiocyanate was added to the solution. The mixture was allowed to shake at room temperature in ultrasonic bath for 10 mins. Acetic water was used to wash and organic solvent evaporated by rotary evaporator.

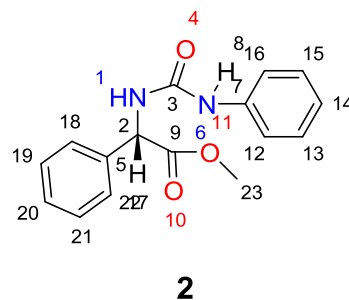
Synthesis of methyl (phenylcarbamoyl)-L-phenylalaninate (1)



A mixture of L-phenyl alanine methyl ester hydrochloride salt (1 g, 4.63 mmol) and Et_3N (0.2 ml, 1.44 mmol) in 5 ml of CH_2Cl_2 , phenylisocyanate (0.2 ml, 2.0 mmol) was slowly added.

Yield= 79.0 %, $[\alpha]_D^{20} = +51.3^\circ$ (0.033 g/5 ml in acetone), HRMS calculated for $C_{17}H_{18}N_2O_3$ m/z [ES]⁻ 321.1225; found 321.1215; 1H -NMR (400 MHz, Chloroform-d): δ 6.39 – 6.28 (m, 7H, Ar), δ 6.23 – 6.19 (m, 2H), Ar), δ 6.15 (td, $J = 7.1, 1.4$ Hz, 1H, Ar), δ 6.01 (s, 1H, NH_8), δ 4.68 (d, $J = 7.9$ Hz, 1H, NH_1), δ 3.94 (dt, $J = 7.9, 6.0$ Hz, 1H, CH), δ 2.83 (s, 3H, CH₃), δ 2.24 (dd, $J = 13.8, 5.7$ Hz, 1H, CHA), δ 2.14 (dd, $J = 13.8, 6.3$ Hz, 1H, CHB). ^{13}C -NMR (101 MHz, d_6 -DMSO): δ 172.9 (C9), δ 154.7 (C3), δ 137.9 (C7), δ 135.7 (C12), δ 129.0 (Ar), δ 128.9 (Ar), δ 128.2 (Ar), δ 126.8 (Ar), δ 123.5 (Ar), δ 120.5 (Ar), δ 53.6 (C2), δ 52.1 (C24), δ 37.9 (C5).

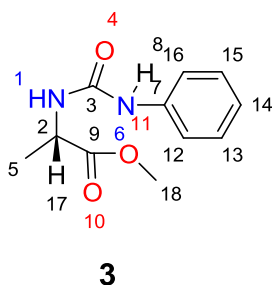
Synthesis of methyl (S)-2-phenyl-2-(3-phenylureido)acetate (2)



A mixture of L-Phenylglycine methylester hydrochloride (1 g, 4.97 mmol) and Et₃N (0.2 ml, 1.44 mmol) in 5 ml of CH₂Cl₂, phenylisocyanate (0.5 ml, 4.2 mmol) was slowly added.

Yield= 28.0 %, $[\alpha]_D^{20} = +35.6^\circ$ (0.15 g/5 ml in acetone), HRMS calculated for C₁₆H₁₆N₂O₃ m/z [ES]⁻ 284.1157; found 284.1161; ¹H-NMR (400 MHz, Chloroform-*d*): δ 7.47 – 7.34 (s, 9H, Ar), δ 7.23 (s, 1H, NH₈), δ 7.01 (m, 1H, Ar), δ 6.37 (broad, s, 1H, NH₁), δ 5.63 (s, 1H, CH), δ 3.75 (s, 3H, OCH₃). ¹³C-NMR (101 MHz, CDCl₃): δ 172.9 (C9), δ 155.3 (C3), δ 138.7 (C7), δ 137.3 (C5), δ 129.7 (Ar), δ 128.9 (Ar), δ 127.6 (Ar), δ 124.2 (Ar), δ 121.2 (Ar), δ 57.6 (C2), δ 53.3 (C23).

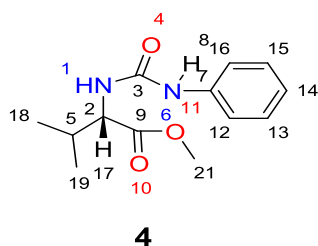
Synthesis of methyl (phenylcarbamoyl)-L-alaninate (3)



L-alanine methyl ester hydrochloride salt (1.0 g, 7.19 mmol) and Et₃N (1.4 ml, 10.75 mmol) in 25 ml of CH₂Cl₂, phenylisocyanate (1.5 ml, 12.56 mmol) was slowly added.

Yield= 47.0 %, $[\alpha]_D^{20} = +72.5^\circ$ (0.06 g/5 ml in acetone), HRMS calculated for C₁₁H₁₄N₂O₃ m/z [ES]⁻ 222.1004; found 222.1004; ¹H-NMR (400 MHz, Chloroform-*d*): δ 7.36 – 7.22 (m, 5H, Ar + 1H, NH₈), δ 7.08 (tt, *J* = 6.8, 1.7 Hz, 1H, Ar), δ 5.85 (broad, s, 1H, NH₁), δ 4.61 (q, *J* = 7.2 Hz, 1H, CH), δ 3.78 (s, 3H, OCH₃), 1.45 (d, 7.2 Hz, 3H, CH₃). ¹³C-NMR (101 MHz, CDCl₃): δ 172.3 (C9), δ 155.9 (C3), δ 138.9 (C7), δ 129.5 (Ar), δ 123.9 (C14), δ 120.9 (Ar), δ 52.9 (C2), δ 49.2 (C18), δ 19.1 (C5).

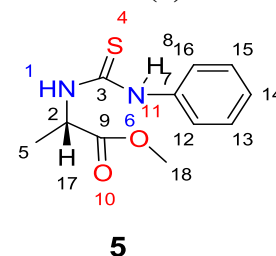
Synthesis of methyl (phenylcarbamoyl)-L-valinate (4)



A mixture of L-valine methyl ester hydrochloride salt (1.0 g, 5.96 mmol) and Et₃N (1.5 ml, 10.76 mmol) in 25 ml of CH₂Cl₂, phenylisocyanate (0.5 ml, 4.2 mmol) was slowly added.

Yield= 40.0 %, M.p. $[\alpha]_D^{20} = +76.3^\circ$ (0.04 g/5 ml in acetone), HRMS calculated for C₁₃H₁₈N₂O₃ m/z [ES]⁻ 250.1317; found 250.1317; ¹H-NMR (400 MHz, Chloroform-*d*): δ 7.14 (s, 1H, NH₈), δ 6.97 – 6.88 (m, 4H, Ar), δ 6.72 – 6.62 (tt, *J* = 6.7, 1.7 Hz, 1H, Ar), δ 5.57 (d, *J* = 8.9 Hz, 1H, NH₁), 4.17 (dd, *J* = 8.8, 4.9 Hz, 1H, CH17), δ 3.38 (s, 3H, OCH₃), δ 1.80 (m, 1H, CH), 0.62 (d, *J* = 6.8 Hz, 3H, CH₃), 0.53 (d, *J* = 6.9 Hz, 3H, CH₃). ¹³C-NMR (101 MHz, CDCl₃): δ 174.1 (C9), δ 156.1 (C3), δ 138.4 (C7), δ 129.2 (2xC, Ar), δ 123.8 (C14), δ 120.8 (2xC, Ar), δ 58.1 (C2), δ 52.3 (C21), δ 31.3 (C5), δ 19.5 (C19), δ 17.9 (C18).

Synthesis of methyl (phenylcarbamothioyl)-L-alaninate (5)



L-Alanine methyl ester hydrochloride (3.3 g, 23.5 mmol) and Et₃N (1.5 ml, 10.76 mmol) in 100 ml of CH₂Cl₂, phenylisocyanate (2 ml, 16.8 mmol) was slowly added.

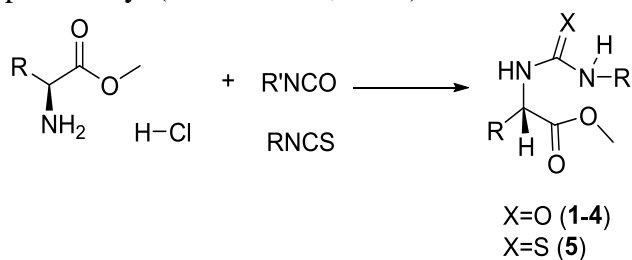
Yield= 60.0 %, $[\alpha]_D^{20} = +41.7^\circ$ (0.15 g/5 ml in acetone), HRMS calculated for C₁₁H₁₄N₂O₂S m/z [ES]⁻ 238.0777; found 238.0776; ¹H-NMR (400 MHz, Chloroform-*d*): δ 8.36 (s, 1H, NH₈), δ 7.55 – 7.20 (m, 5H, Ar), δ 6.76 (d, *J* = 7.5 Hz, 1H, NH₁), δ 5.19 (p, *J* = 7.2 Hz, 1H, CH), δ 3.78 (s, 3H, OCH₃), 1.45 (dd, 7.2, 1.0 Hz, 3H, CH₃). ¹³C NMR (101 MHz, CDCl₃): δ 180.1 (C3), δ 174.1 (C9), δ 136.4 (C7), δ 130.6 (2XC, Ar), δ 127.7 (C14), δ 125.2 (2XC, Ar), δ 53.8 (C2), δ 53.1 (C18), δ 18.9 (C5).

3. Discussion

3.1. Chemistry

In this study, different substituted esters of hydantoic and thiohydantoic acids were synthesized by the reaction of corresponding optically active amino acids methyl ester hydrochloride with substituted isocyanate/isothiocyanate in the presence of triethylamine. To avoid racemisation (Ballard *et*

al., 2019) amount of triethylamine and reaction time has been decreased. (Scheme 2) 5,5-disubstituted hydantoin were synthesized previously (Jawhar *et al.*, 2018)



Scheme 2: Synthesis of compound 1-5

All synthesized compounds have been characterized by ^1H -NMR and ^{13}C -NMR spectra. The ^1H -NMR spectra of compounds **2**, and **3** showed a broad singlet at δ 6.37, 5.85 ppm, respectively due to NH group in the compound. While, the ^1H -NMR spectra of compounds **1**, and **4** showed doublet at δ 4.68 ppm (d, $J = 7.9$ Hz, 1H, NH) and δ 5.7 ppm (d, $J = 8.9$ Hz, 1H, NH), respectively due to the hydrogen attached to the stereogenic centre. Hydrogen attached to the stereogenic centre showed doublet triplet at δ 3.94 ppm with $J = 7.9, 6.0$ Hz, and doublet doublet at δ 4.17 with $J = 8.8, 4.9$ Hz for compounds **1**, and **4**, respectively.

The ^{13}C -NMR spectrum showed peaks which are in agreement with number of chemically equivalent carbons present in all compounds.

3.2 Energy profile

To determine insight into the energy behavior between the compounds, selected physicochemical parameters were also calculated using B3LYP functional basis methods. (Table 1) Table 1 shows different negative values of energy based on the aromatic and aliphatic substituents on the chiral position. Energy values for compounds **3** and **5** are approximately not far from each other because of their similarity in molecular structure attached to Chiral center with C=O and C=S difference. Energy profile values have been determined by the Hartree-Fock and B3LYP functional basis set for all atoms for **1-5**. (Table 1)

Table 1: Energy profile (in kcal/mol)

Energy/ kcal/mol		
6-31G		
Compounds	Hartree-Fock	B3LYP
1	-612790.21	-623560.62
2	-585692.07	-592487.81
3	-692899.44	-473199.81
4	-517611.70	-520857.24
5	-672830.49	-675972.48

3.3 Frontier Molecular Orbital (FMO) Analysis

Difference of energy between lowest unoccupied molecular orbital (LUMO) and highest occupied molecular orbital (HOMO) in gas phase at the B3LYP level is an important factor to calculate molecular reaction potentials (Fareghi- Alamdari *et al.*, 2015)

The B3LYP method and basis set of 6-31G has been used to obtain E_{HOMO} , E_{LUMO} and LUMO-HOMO energy gap (Eg; Δ) of compounds **1-5**. Molecular orbital properties such as energy and frontier electron density are essential to give molecular reactivity information. Figure 1 shows values of HOMO energy (E_{HOMO}) and the LUMO energy (E_{LUMO}) of **1** is -0.31 eV and -0.017 eV, respectively. The energy of the HOMO is mainly related on the ionization potential and focused around carbonyl and nitrogen attached to the phenyl ring. While, the electron affinity can be observed by LUMO energy which is focused on benzyle attached to the chiral position. The differences of energy between both molecular orbital $E_{\text{LUMO-HOMO}}$ calculated as a small value 0.14 eV for compound **1** is simply show higher reactivity compare with compounds **2,3** and **4**.

LUMO-HOMO energy gap for compound **2** shows 0.16 eV indicates less reactive compare with the other synthesized compounds. LUMO-HOMO energy gap for compounds **3** and **4** show values of 0.15 and 0.15 eV respectively, which observe similar softness and reactive compounds. A value of 0.10 eV is a LUMO-HOMO energy gap for compound **5** show high reactive compound compare with other synthesized compounds. (See supporting information) Hence, we can conclude synthesized compounds in order

of increasing reactivity based on LUMO-HOMO energy gap as follows; $5 > 1 > 3$, $4 > 2$. The HOMO for all synthesized compounds is mostly located along the carbonyl and substituent attached to nitrogen. The LUMO is mostly located over the groups attached to the stereogenic center.

Recently, Koopman's theory has been used to calculate ionization potential for different compounds by Chong *et al.* (Chong *et al.*, 2002) using orbital energies which is equal to a negative value of HOMO energy ($IP = -E_{HOMO}$). A negative value of LUMO energy is equal to electron affinity ($EA = -E_{LUMO}$) (Shankar *et al.*, 2009, Rocha *et al.*, 2015). The chemical hardness η of the molecule based on the molecular orbital can be calculated by the following equation (equation 1) (Galván *et al.*, 2015)

$$\eta = \left(\frac{E_{LUMO} - E_{HOMO}}{2} \right) \quad \text{Equation 1}$$

While, electro negativity χ can be obtained by equation 2

$$\chi = -\frac{E_{LUMO} + E_{HOMO}}{2} \quad \text{Equation 2}$$

Hence, Chemical hardness η is equal to the energy gap between LUMO and HOMO divided by two and the half-way between the LUMO and HOMO corresponds to electro negativity χ of the molecule. Hardness η and softness s values give information of the molecule about reactivity and stability. Therefore, Other chemical properties can be calculated by using LUMO and HOMO energy values for instance; hardness $\eta = IP - EA / 2$, electrophilicity index $\omega = \mu^2 / 2\eta$, electro-negativity $\chi = IP + EA / 2$, chemical potential $\mu = -\chi$, softness $s = 1/2\eta$ and. (Rocha *et al.*, 2015) (Table 2) Table 2 shows small values of $E_{LUMO-HOMO}$ gap indicating a soft molecule, more reactive, and higher polarizable compound than high values of $E_{LUMO-HOMO}$. Values also show that the compound can easily decompose spontaneously to its elements. (Rao *et al.*, 2016)

Table 2: Reactivity properties, HOMO and LUMO energies, HOMO–LUMO energy gap of 1.

Molecular parameters	B3LYP/6-31G
EHOMO (eV)	-0.31
ELUMO (eV)	-0.17
$\Delta E_{LUMO-HOMO}$ (eV)	0.14
Ionization potential, IP (eV)	0.31
Electron affinity, EA (eV)	0.17
Electronegativity, χ (eV)	0.24
Chemical potential, μ (eV)	-0.24
Chemical hardness, η (eV)	0.07
Chemical softness, s (eV ⁻¹)	7.14
Global electrophilicity index ω	0.41

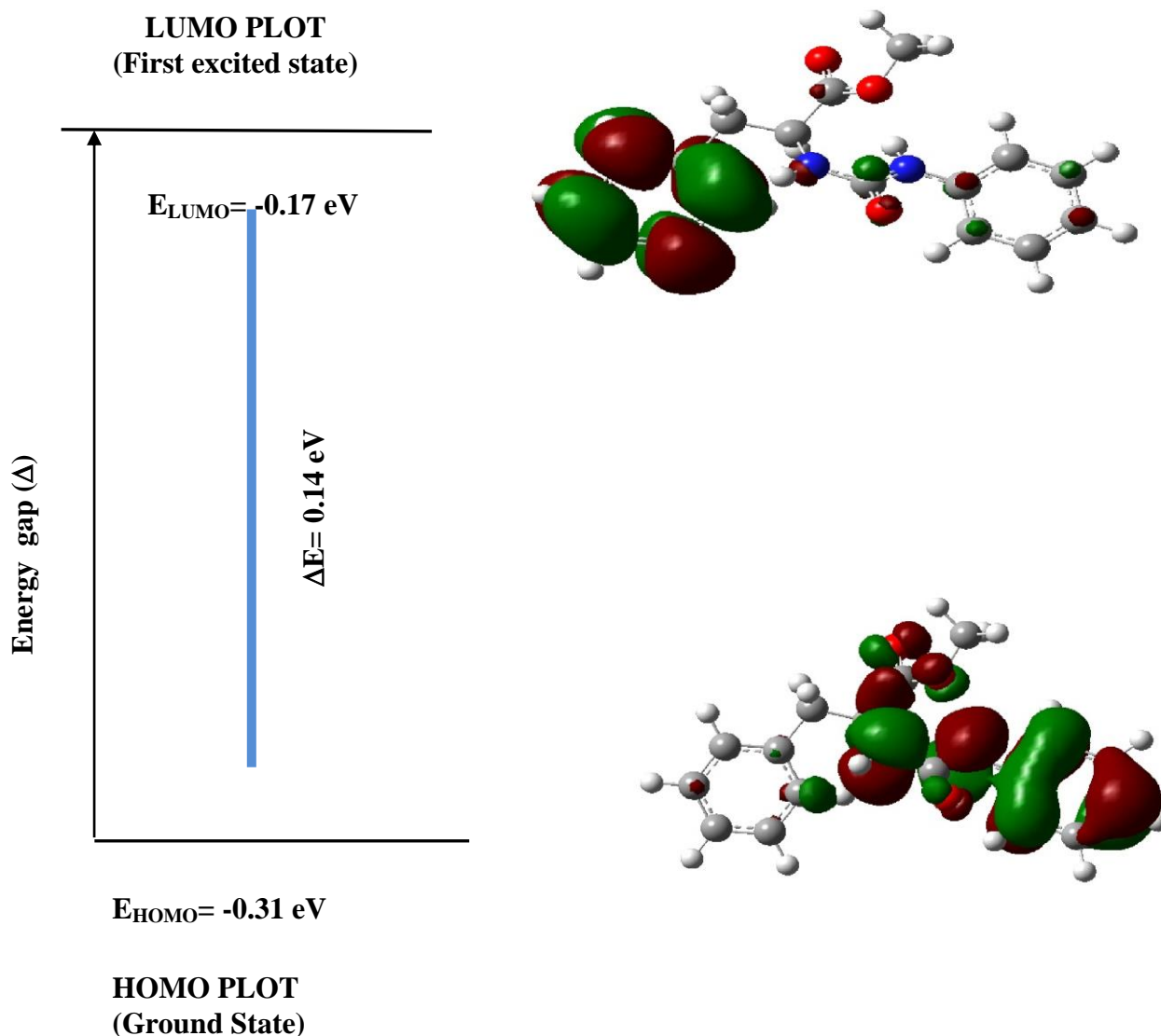


Figure 1: Molecular orbitals and LUMO and HOMO energy gap of **1**

3.4 Molecular electrostatic potential

The molecular electrostatic potential (MEP) is a tool to give a good correlation between physicochemical properties and molecular structure reactivity to express binding site of drug and nucleophile and electrophile position of the molecule. (Scrocco and Tomasi, 1978) (Rao et al., 2016). Red color region in Figure 2 for compound **5** shows a maximum electron density which is cover phenyl attached to the nitrogen, C=O, and

sulfur. Electron density lowest region (Blue color) corresponds to the hydrogen atoms bound to the methyl on the chiral centre and oxygen of ester, and carbon attached to the nitrogen. (Kubinyi *et al.*, 2006, Moro *et al.*, 2005) (Figure 2) Molecular electrostatic potential surface for compounds **1-4** represent variety of electron distribution with different color areas. (See supporting information Figure S14-17)

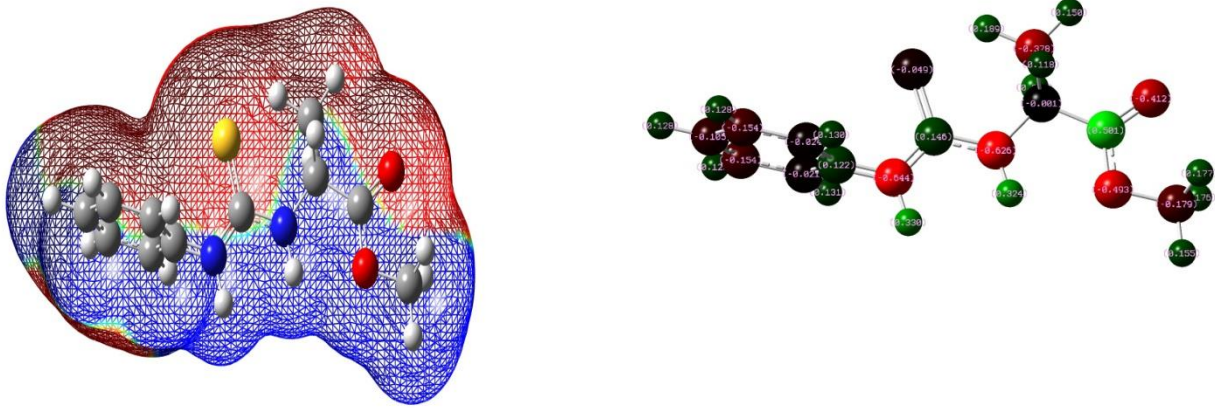
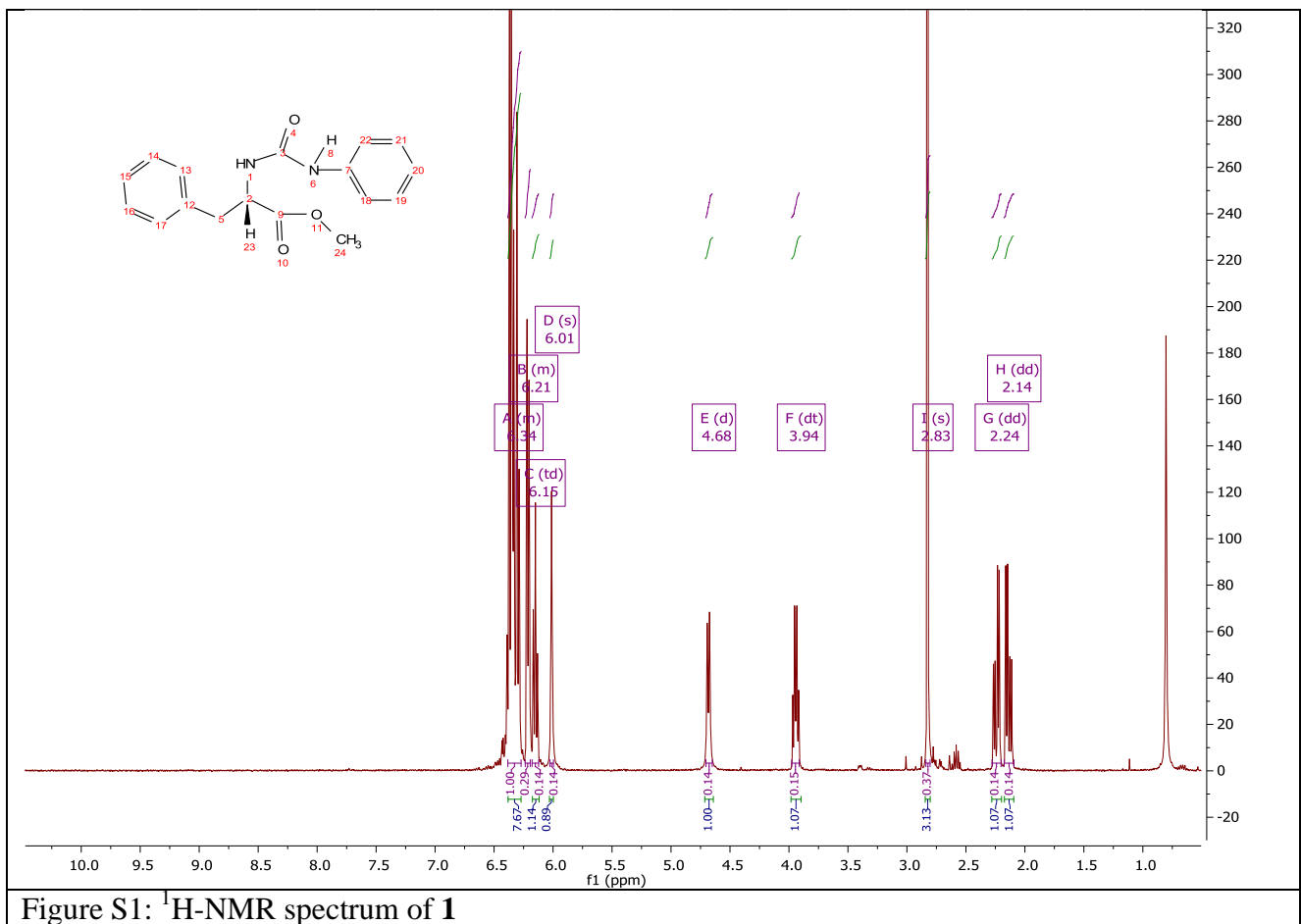


Figure 2: Molecular electrostatic potential surface and charge distribution value for compound 5.



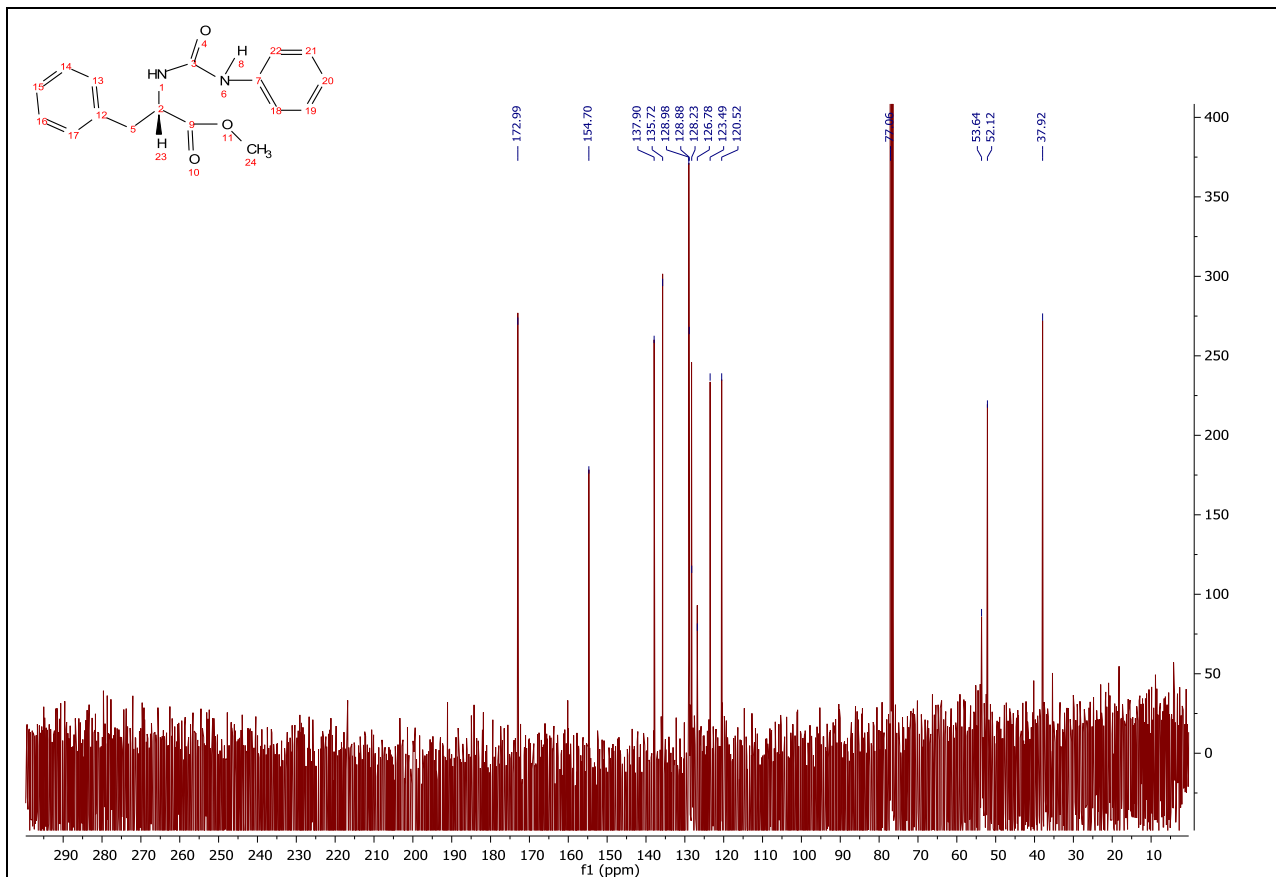


Figure S2: ¹³C -NMR spectrum of **1**

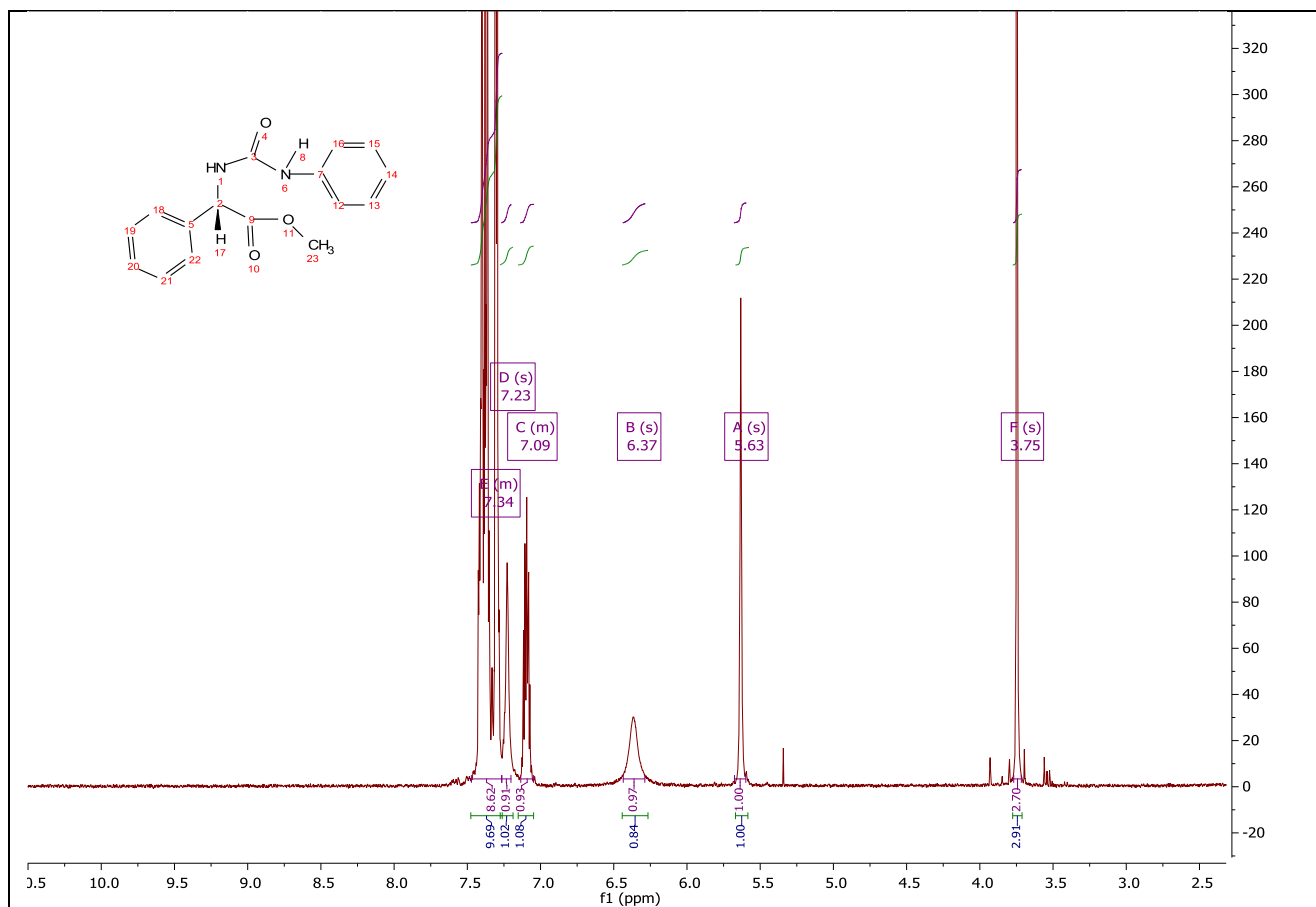
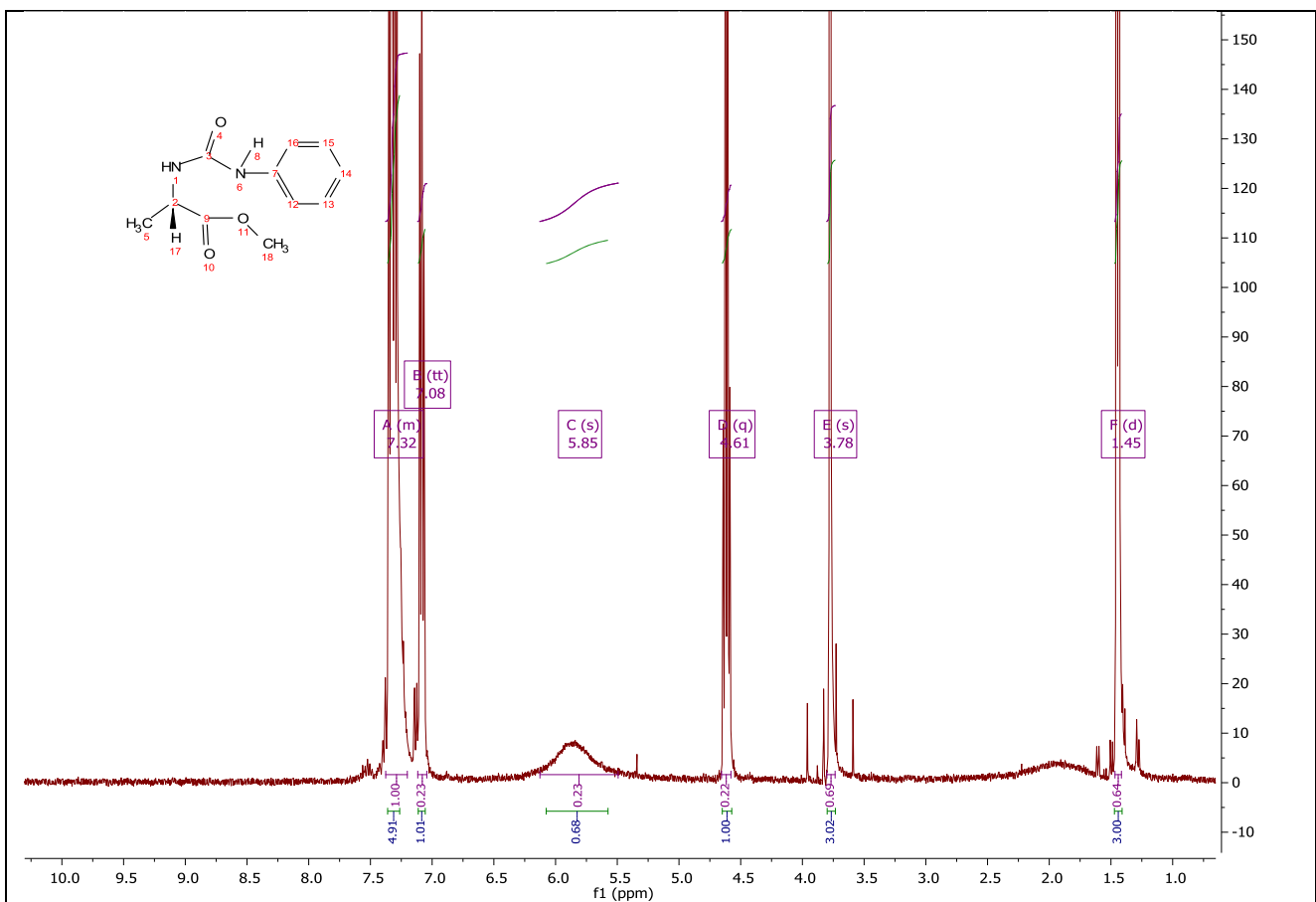
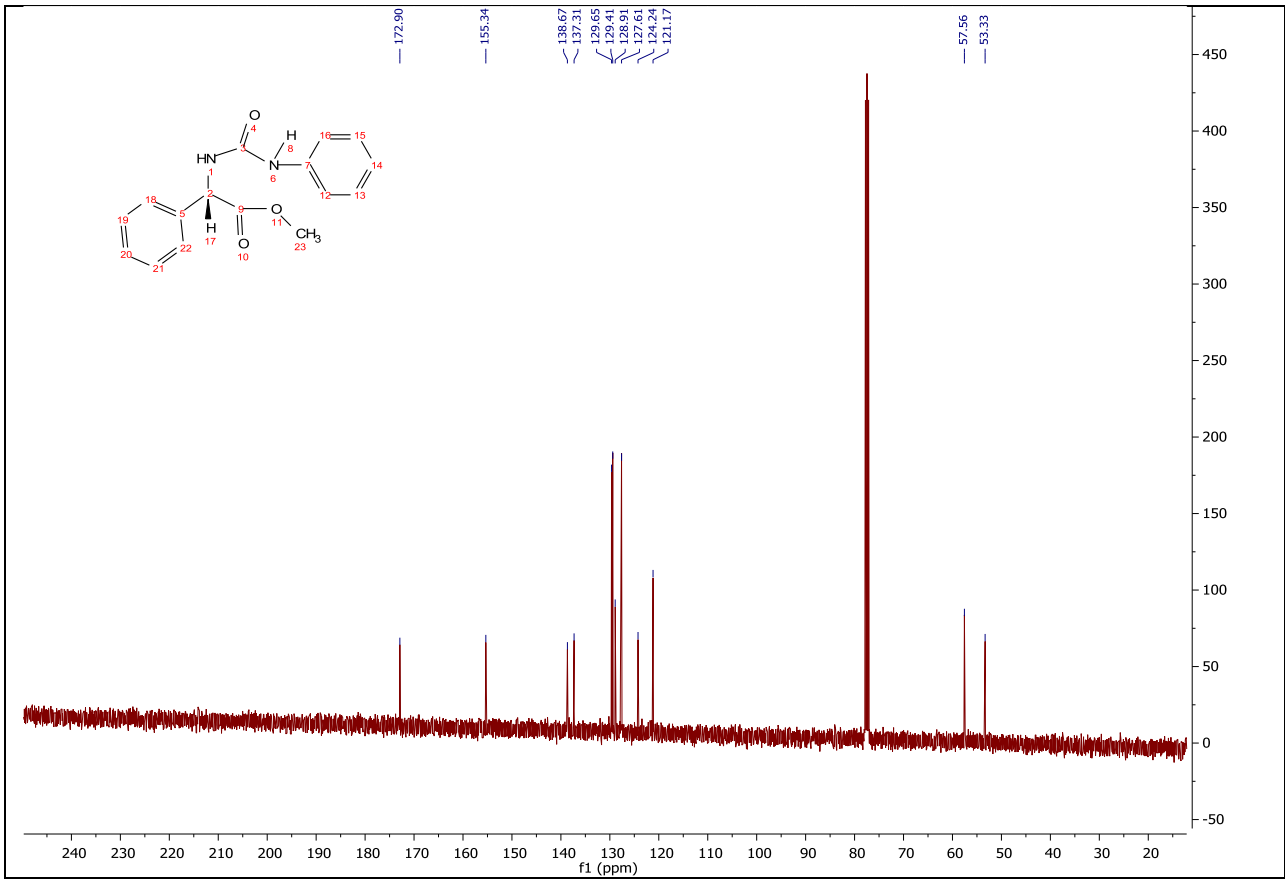
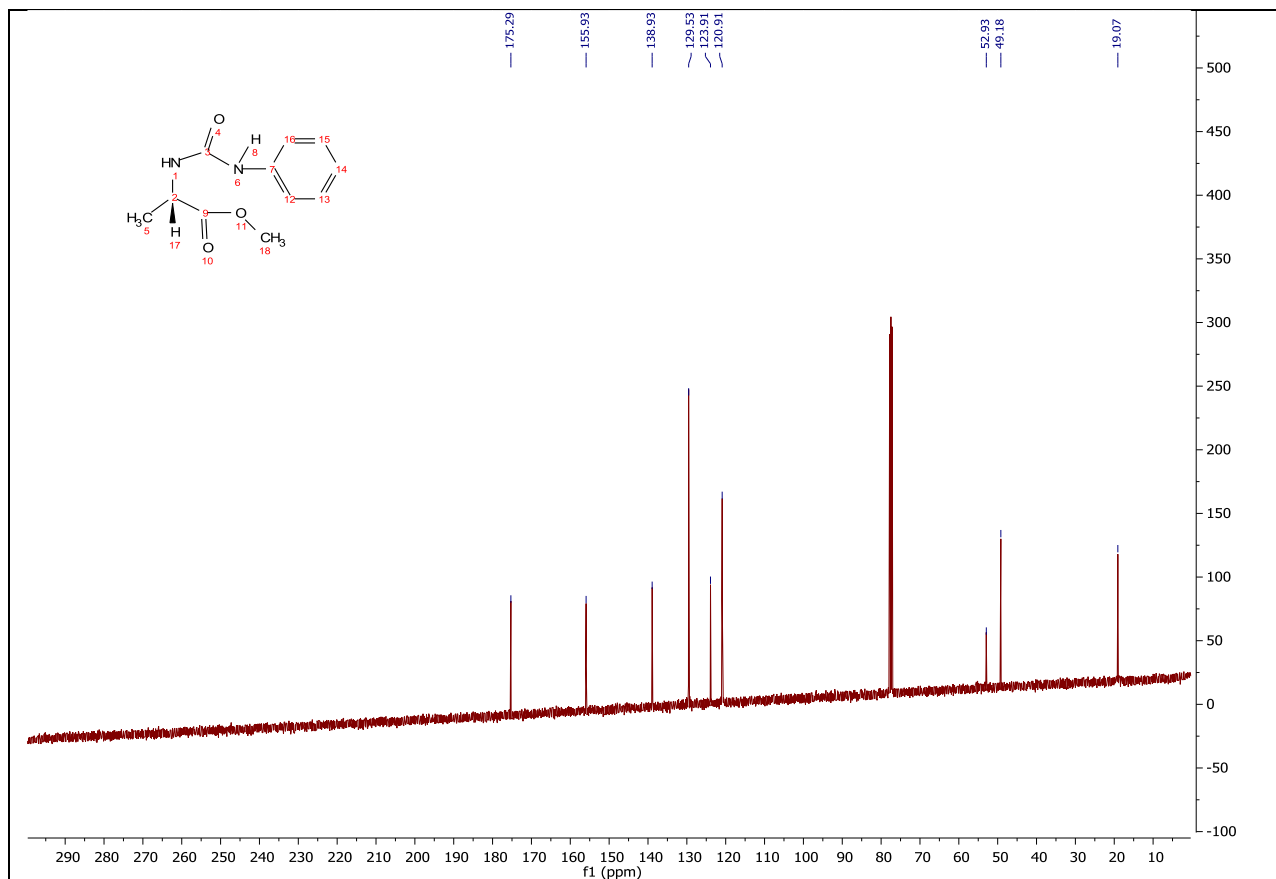
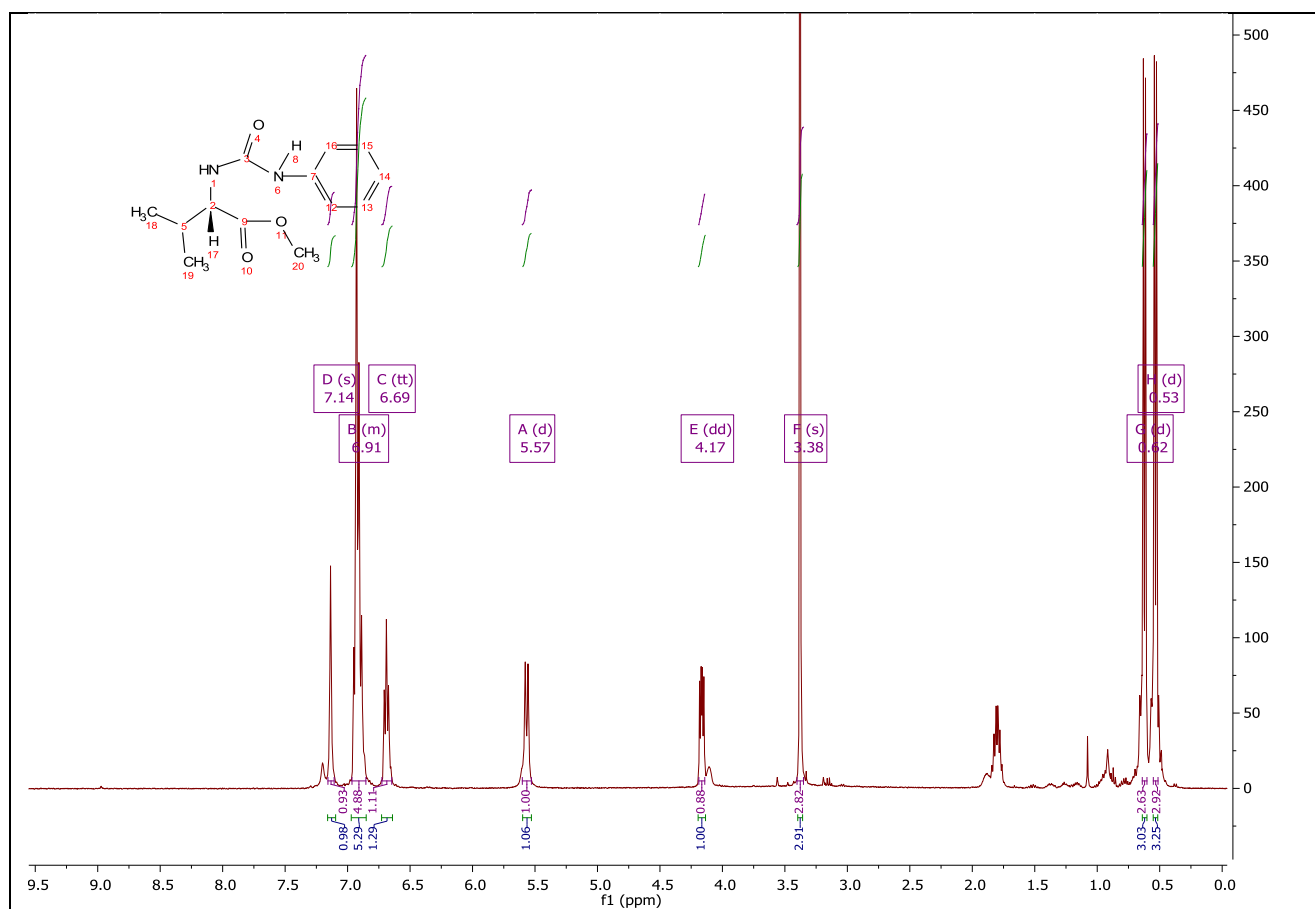
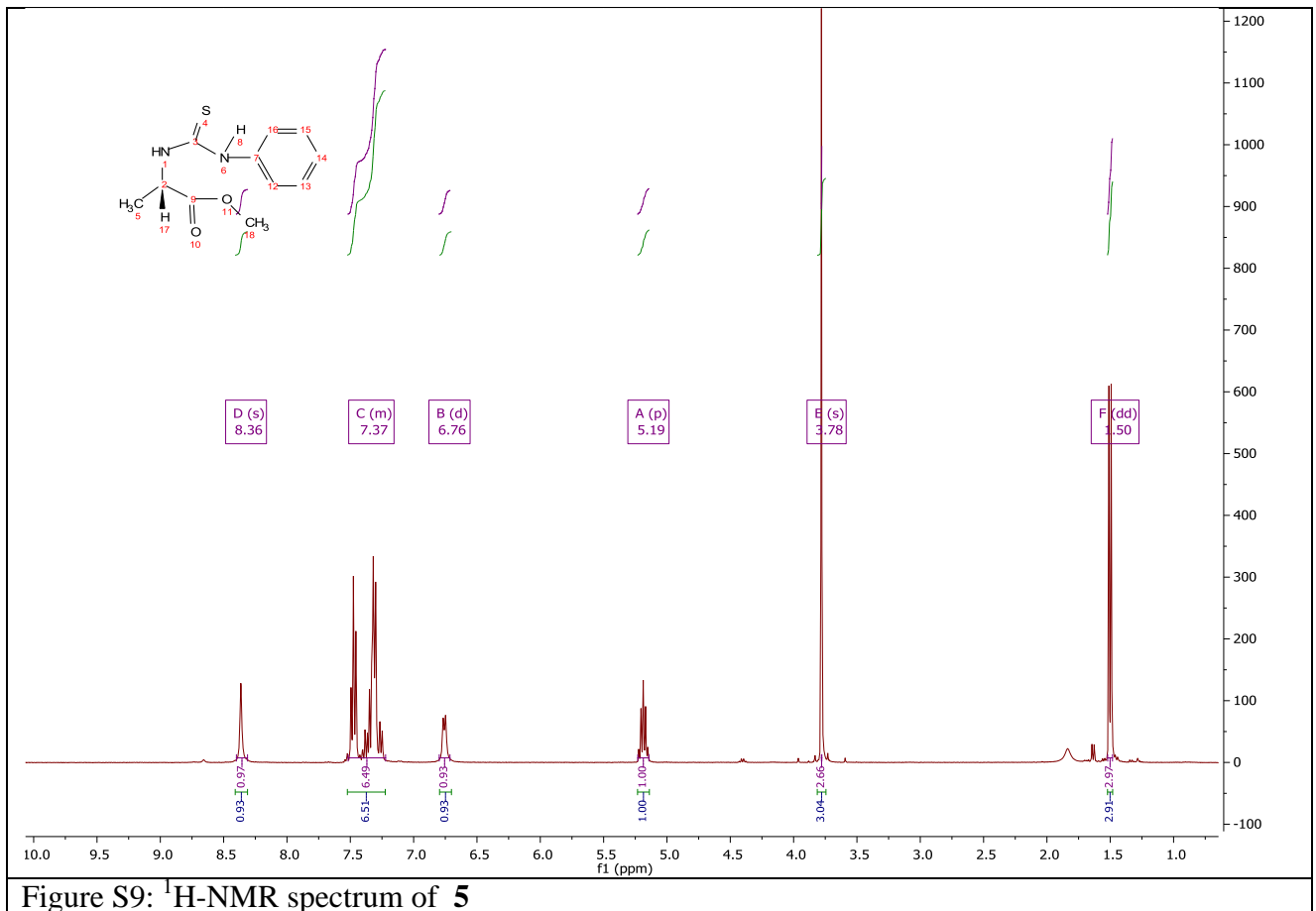
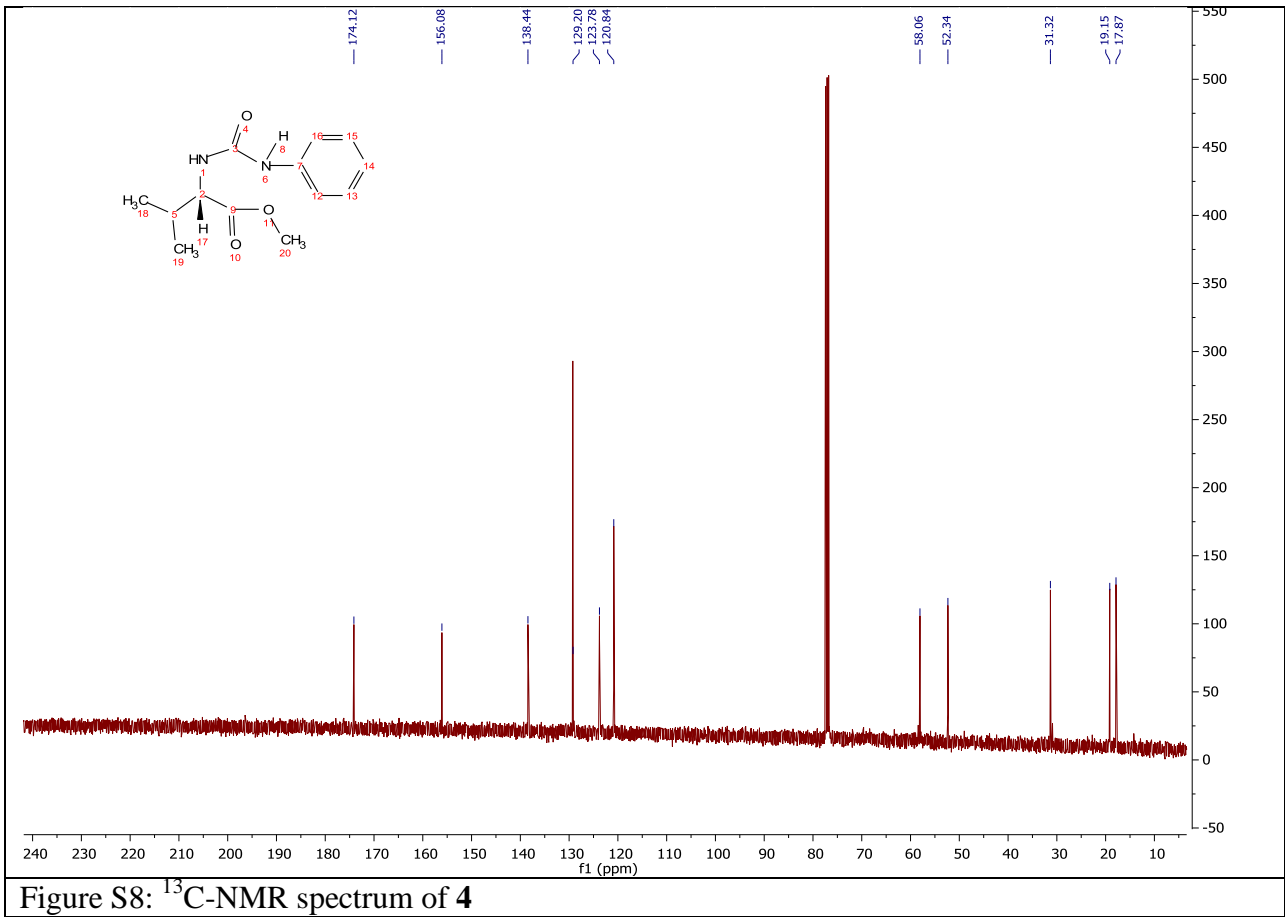
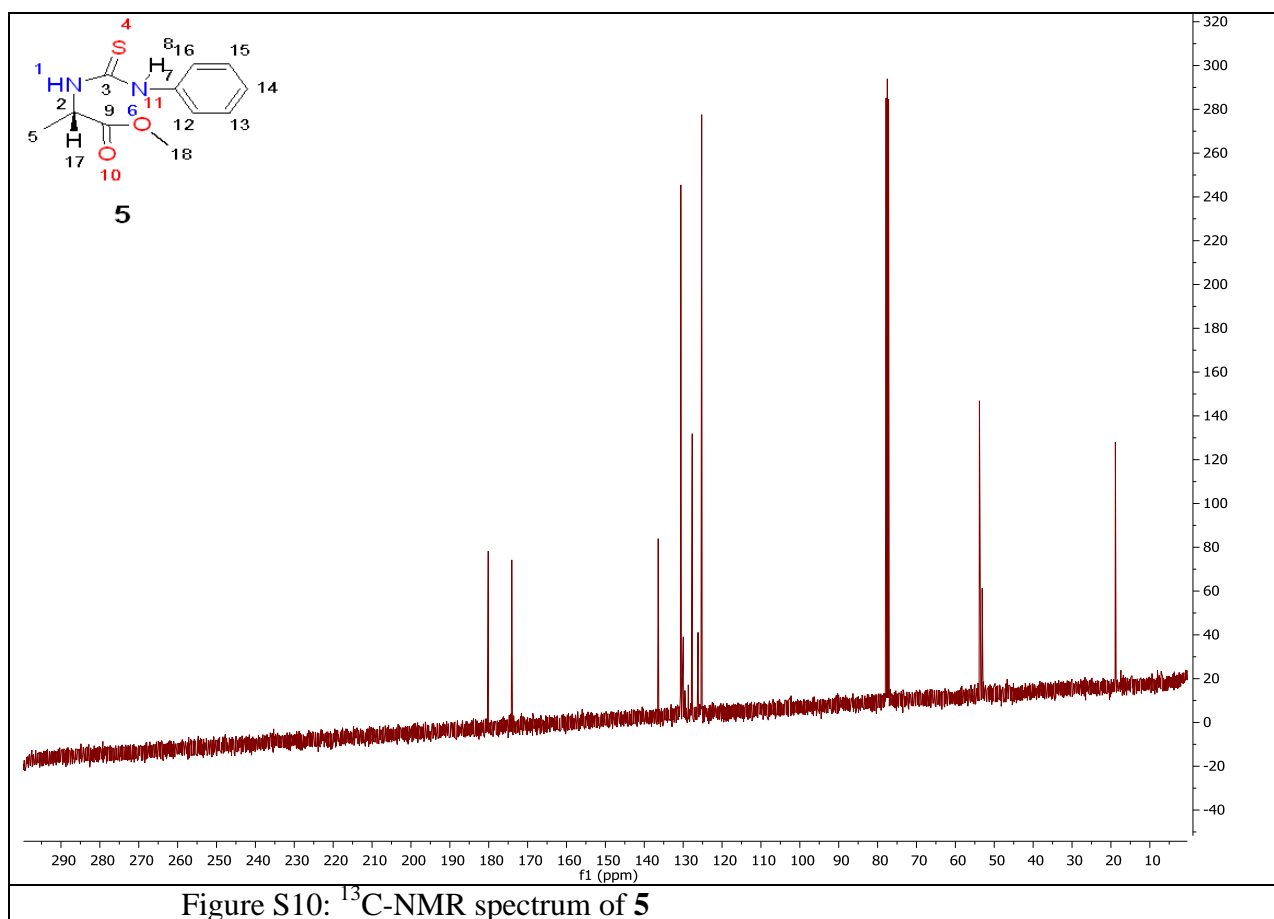


Figure S3: ¹H- NMR spectrum of **2**



Figure S6: ^{13}C -NMR spectrum of 3Figure S7: ^1H -NMR spectrum of 4





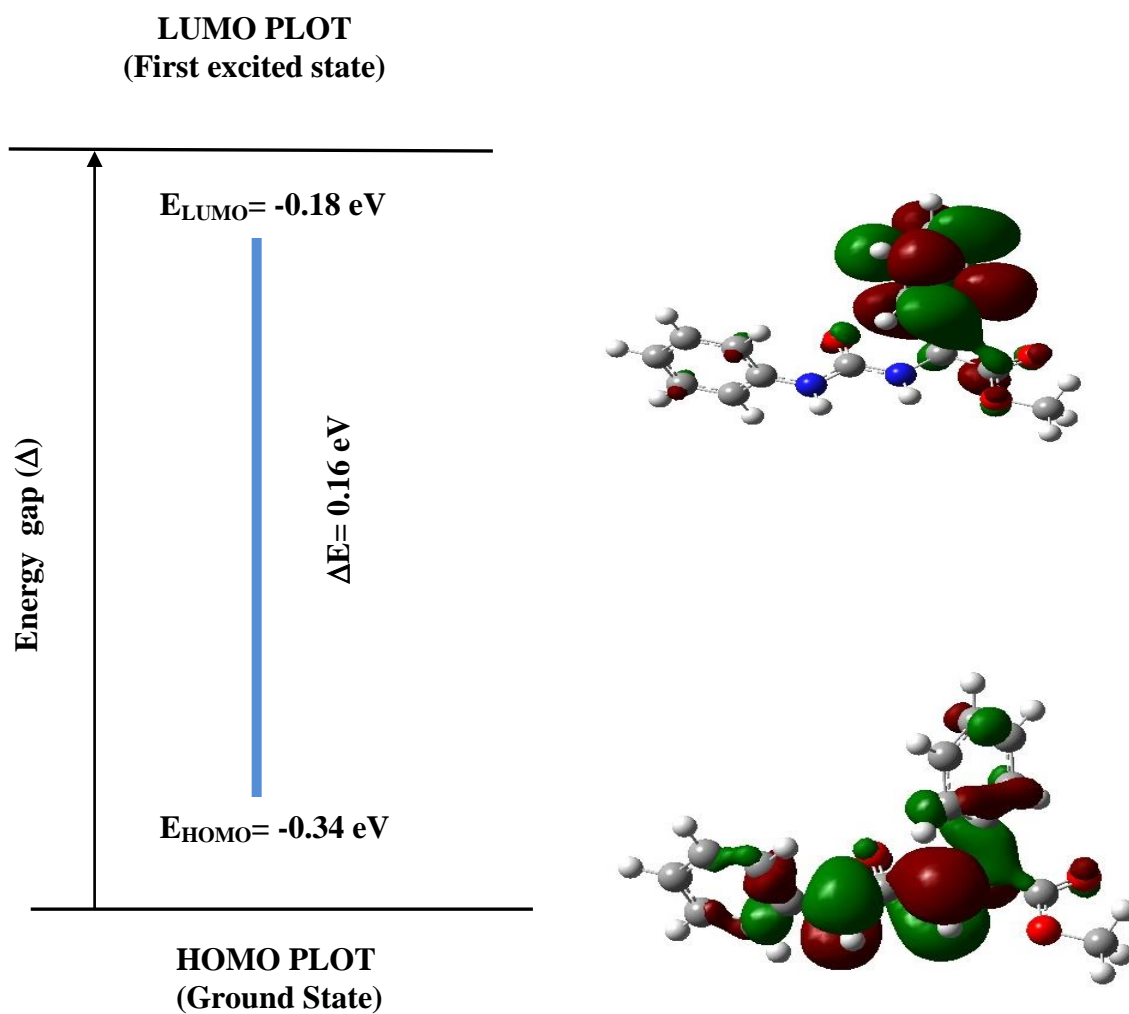


Figure S11: Frontier molecular orbitals of **2** (Δ : Energy gap between LUMO and HOMO)

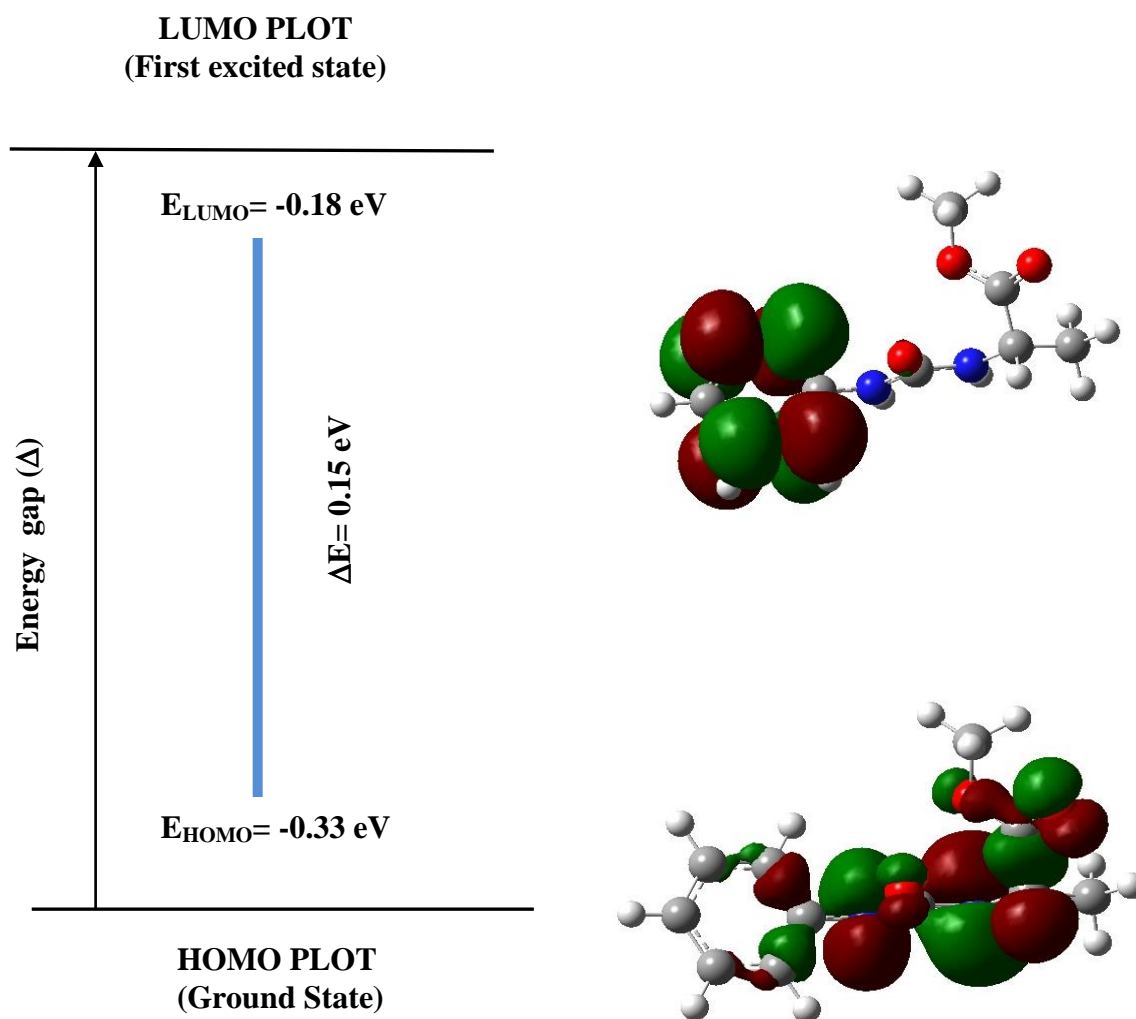


Figure S12: Frontier molecular orbitals of **3** (Δ : Energy gap between LUMO and HOMO)

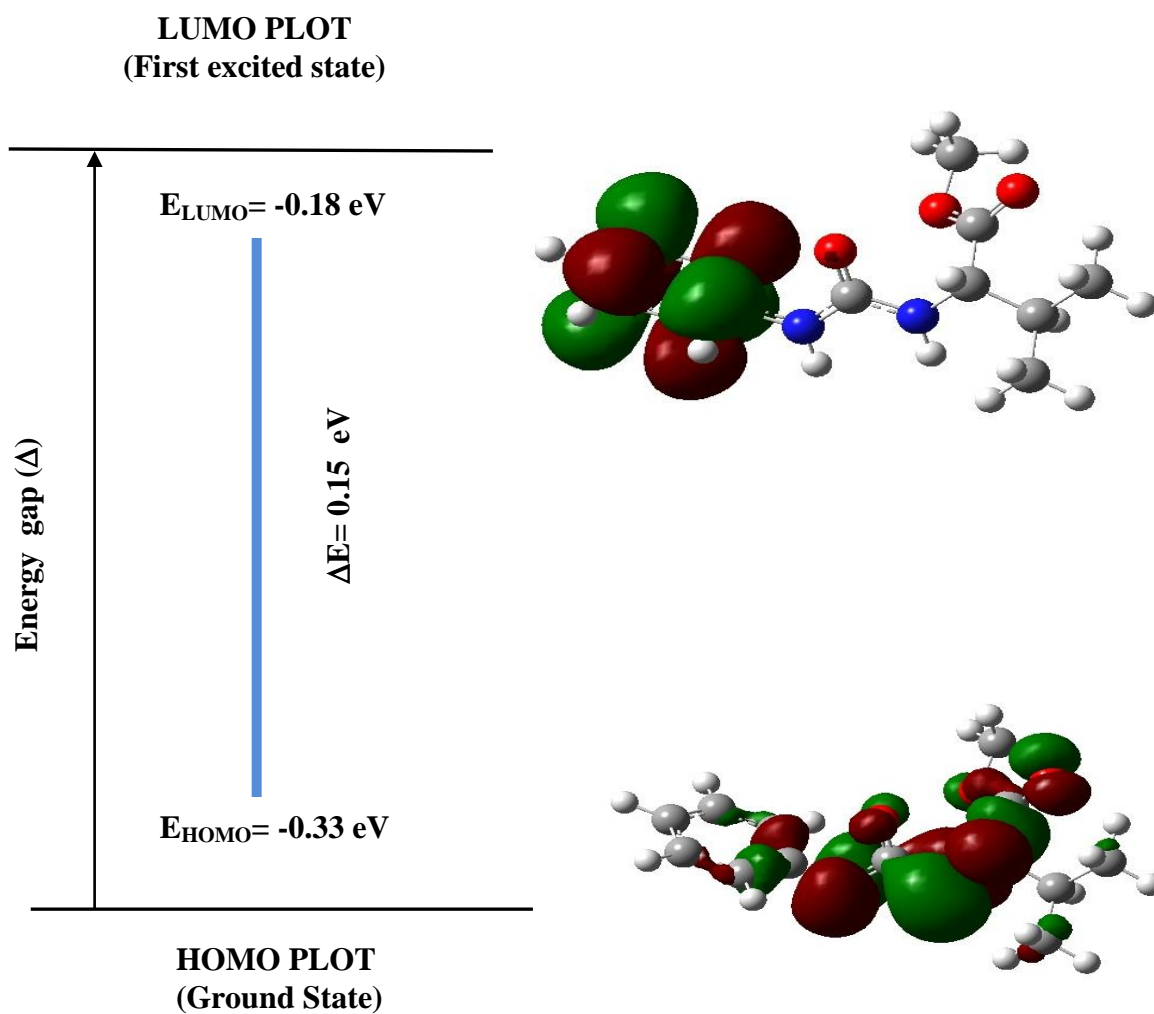


Figure S13: Frontier molecular orbitals of **4** (Δ : Energy gap between LUMO and HOMO)

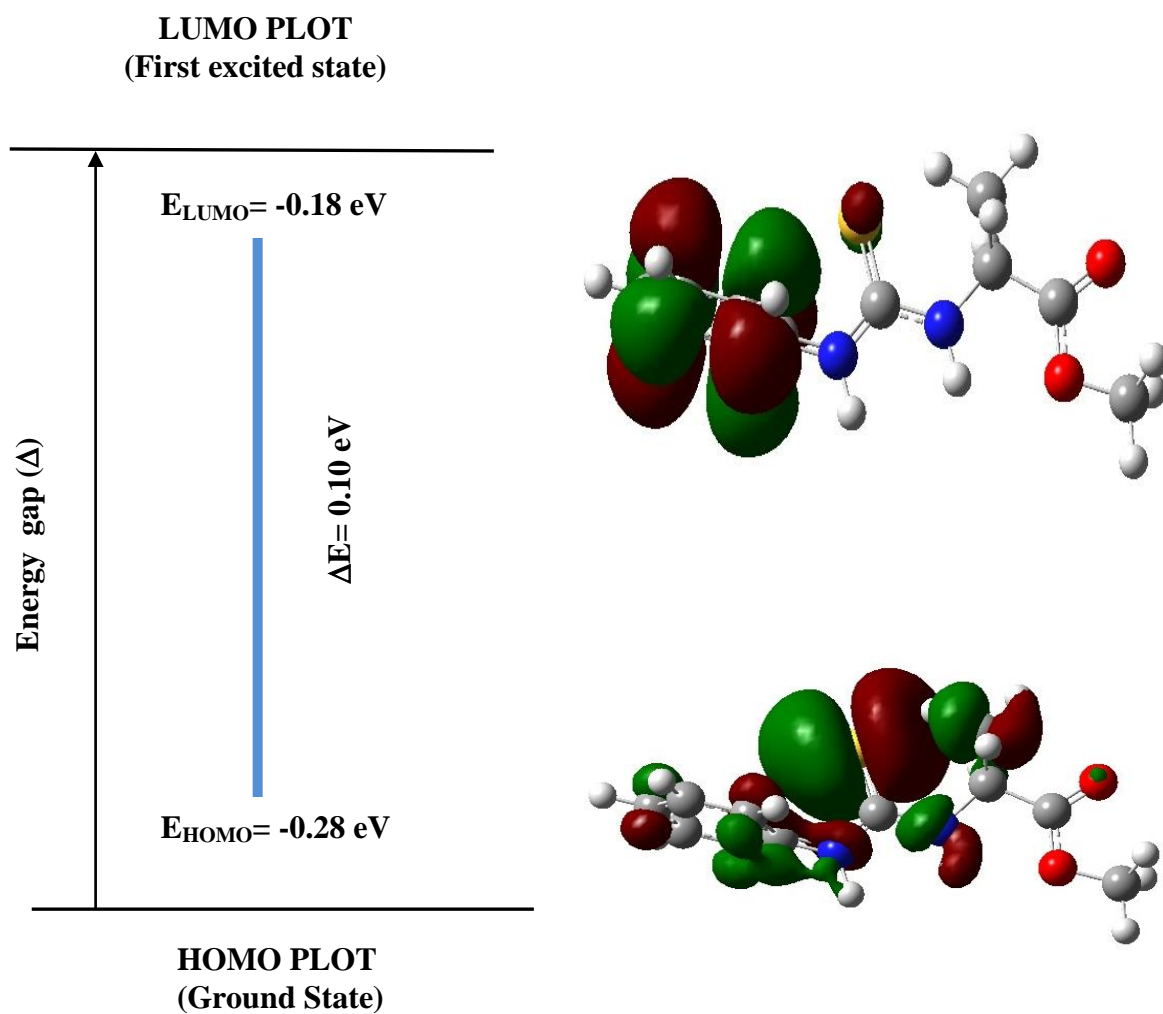


Figure S14: Frontier molecular orbitals of **5** (Δ : Energy gap between LUMO and HOMO)

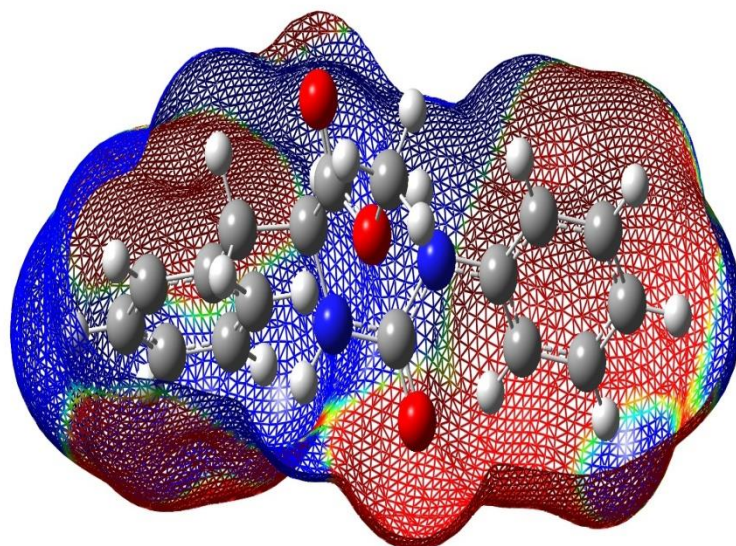


Figure S15: Molecular electrostatic potential for compound **1**.

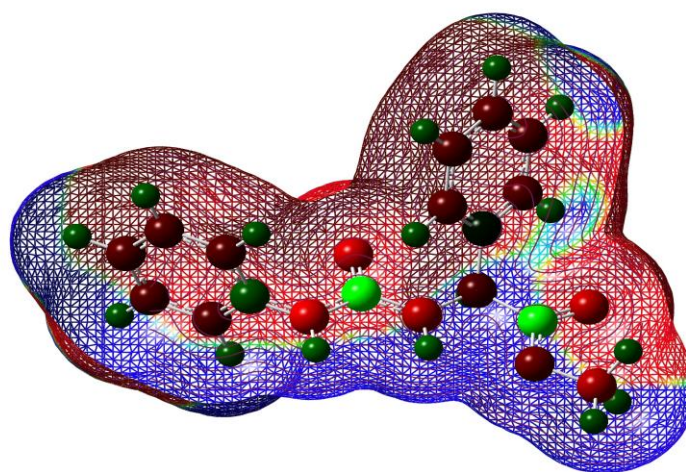


Figure S16: Molecular electrostatic potential for compound **2**.

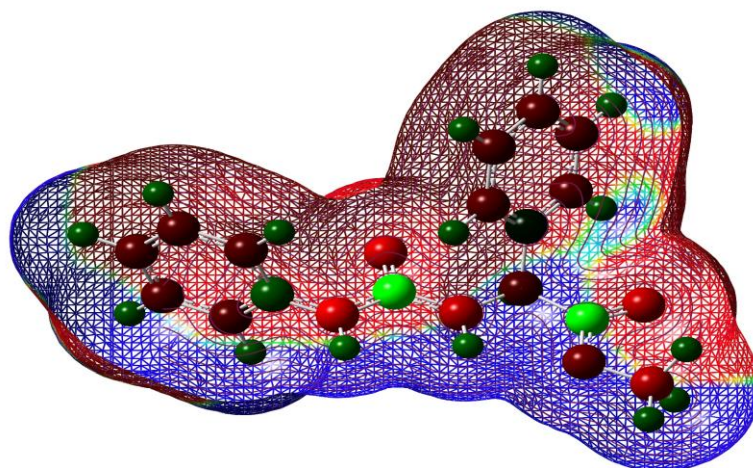


Figure S17: Molecular electrostatic potential for compound **3**.

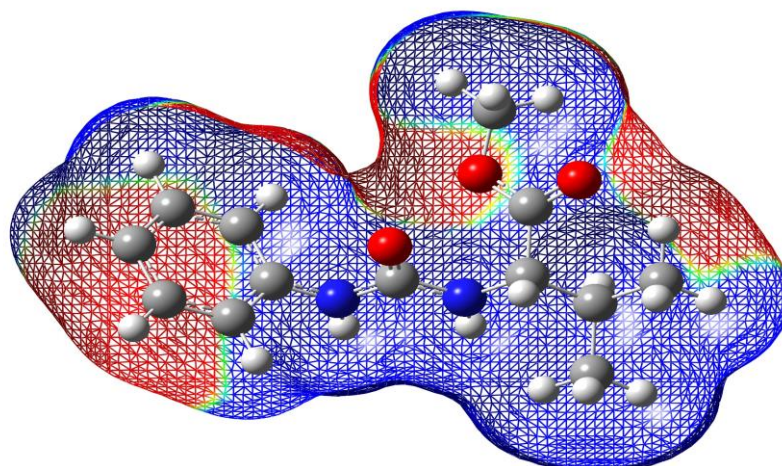


Figure S18: Molecular electrostatic potential for compound **4**.

3.5 Thermodynamic parameters

Thermodynamic parameters for all synthesized compounds have been calculated by using B3LYP/6-31G level in Gaussian 09 W. All values such as Molar heat capacity constant volume (C_v) (Abdullah et al., 2016), relative energy (E),

enthalpies (ΔH), entropies (S) and Gibbs free energy (ΔG) are shown in Table 3.

Table 4 shows negative values of relative energy, Gibbs free energy and enthalpies of **1-5**.

Compounds	E(kcal/mol)	ΔG (kcal/mol)	ΔH (kcal/mol)	S(cal/molK)	C_v (cal/molK)
1	217.728	-623483	-623437	155.739	76.097
2	198.920	-598831	-598787	148.857	71.195
3	163.752	-478544	-478505	131.711	58.136
4	201.128	-527850	-527807	144.993	68.439
5	162.432	-681201	-681161	134.346	59.307

corona virus (MERS-Co). *ZANCO Journal of Pure and Applied Sciences*, 31, 71-78.

Conclusions

Different substituted esters of hydantoic and thiohydantoic acids have been synthesized with optical active properties. A complete structural, NMR, Mass and thermodynamic parameters have been calculated for compounds **1-5**. The relatively low value of $E_{LUMO-HOMO}$ gap indicates low chemical stability and high reactivity of compounds **1-5**. The positive values of thermodynamic parameters suggest high reactivity of compounds **1-5**. The differences of energy between both molecular orbitals $E_{LUMO-HOMO}$ calculated as a small value 0.10 eV for compound **5** which simply shows higher reactivity than the other compounds mentioned in this study.

LUMO-HOMO energy gap for compound **2** shows 0.16 eV indicates less reactive compound in comparison with other synthesized compounds. LUMO-HOMO energy gap for compounds **3**, and **4** show values of 0.15, and 0.15 eV, respectively which observe approximately similar softness and reactive compounds. A value of 0.14 eV is a LUMO-HOMO energy gap for compound **1** show less reactive than compound **5** and more reactive than other synthesized compounds. Hence, we can conclude synthesized compounds in order of increasing reactivity based on LUMO-HOMO energy gap as follows ; **5**>**1**>**3**, **4**>**2**.

4. References

ABDALLAH, H. 2019. Theoretical study for the inhibition ability of some bioactive imidazole derivatives against the Middle-East respiratory syndrome

ABDULLAH, B. J., OMAR, M. S. & JIANG, Q. J. 2016. Grüneisen Parameter and Its Related Thermodynamic Parameters Dependence on Size of Si Nanoparticles. *ZANCO Journal of Pure and Applied Sciences*, 28, 126-132.

BALLARD, A., AHMAD, H. O., NARDUOLO, S., ROSA, L., CHAND, N., COSGROVE, D. A., VARKONYI, P., ASAAD, N., TOMASI, S. & BUURMA, N. J. 2018. Quantitative prediction of rate constants for aqueous racemization to avoid pointless stereoselective syntheses. *Angewandte Chemie*, 130, 994-997.

BALLARD, A., NARDUOLO, S., AHMAD, H. O., COSGROVE, D. A., LEACH, A. G. & BUURMA, N. J. 2019. The problem of racemization in drug discovery and tools to predict it. *Expert opinion on drug discovery*, 14, 527-539.

BECKE, A. D. 1993. Density- functional thermochemistry. III. The role of exact exchange. *The Journal of chemical physics*, 98, 5648-5652.

CHONG, D., GRITSENKO, O. & BAERENDS, E. 2002. Interpretation of the Kohn–Sham orbital energies as approximate vertical ionization potentials. *The Journal of Chemical Physics*, 116, 1760-1772.

FAREGHI- ALAMDARI, R., ZANDI, F. & KESHAVARZ, M. H. 2015. A new model for prediction of one electron reduction potential of nitroaryl compounds. *Zeitschrift für anorganische und allgemeine Chemie*, 641, 2641-2648.

FRISCH, A., NIELSON, A. & HOLDER, A. 2000. Gaussview user manual. *Gaussian Inc., Pittsburgh, PA*, 556.

- FRISCH, M. J., TRUCKS, G. W., SCHLEGEL, H. B., SCUSERIA, G. E., ROBB, M. A., CHEESEMAN, J. R., SCALMANI, G., BARONE, V., PETERSSON, G. A., NAKATSUJI, H., LI, X., CARICATO, M., MARENICH, A. V., BLOINO, J., JANESKO, B. G., GOMPERTS, R., MENNUCCI, B., HRATCHIAN, H. P., ORTIZ, J. V., IZMAYLOV, A. F., SONNENBERG, J. L., WILLIAMS, DING, F., LIPPARINI, F., EGIDI, F., GOINGS, J., PENG, B., PETRONE, A., HENDERSON, T., RANASINGHE, D., ZAKRZEWSKI, V. G., GAO, J., REGA, N., ZHENG, G., LIANG, W., HADA, M., EHARA, M., TOYOTA, K., FUKUDA, R., HASEGAWA, J., ISHIDA, M., NAKAJIMA, T., HONDA, Y., KITAO, O., NAKAI, H., VREVEN, T., THROSELL, K., MONTGOMERY JR., J. A., PERALTA, J. E., OGLIARO, F., BEARPARK, M. J., HEYD, J. J., BROTHERS, E. N., KUDIN, K. N., STAROVEROV, V. N., KEITH, T. A., KOBAYASHI, R., NORMAND, J., RAGHAVACHARI, K., RENDELL, A. P., BURANT, J. C., IYENGAR, S. S., TOMASI, J., COSSI, M., MILLAM, J. M., KLENE, M., ADAMO, C., CAMMI, R., OCHTERSKI, J. W., MARTIN, R. L., MOROKUMA, K., FARKAS, O., FORESMAN, J. B. & FOX, D. J. 2016. Gaussian 16 Rev. B.01. Wallingford, CT.
- GALVÁN, J. E., GIL, D. M., LANÚS, H. E. & ALTABEF, A. B. 2015. Theoretical study on the molecular structure and vibrational properties, NBO and HOMO–LUMO analysis of the POX3 (X= F, Cl, Br, I) series of molecules. *Journal of Molecular Structure*, 1081, 536-542.
- JAWHAR, Z. S., AHMAD, H. O., HAYDAR, A. A., ABDULLAH, H. A. & MAHAMAD, S. A. 2018. One-Pot Synthesis, Pharmacological Evaluation, Docking Study, and DFT Calculations for Selected Imidazolidine-2, 4-Diones. *Science Journal of University of Zakho*, 6, 150-154.
- KUBINYI, H., FOLKERS, G. & MARTIN, Y. C. 2006. *3D QSAR in drug design: recent advances*, Springer Science & Business Media.
- LOMBARDINO, J. G. & GERBER, C. F. 1964. Preparation and hypoglycemic activity of some 3, 5-disubstituted hydantoins. *Journal of Medicinal chemistry*, 7, 97-101.
- MORO, S., BACILIERI, M., FERRARI, C. & SPALLUTO, G. 2005. Autocorrelation of molecular electrostatic potential surface properties combined with partial least squares analysis as alternative attractive tool to generate ligand-based 3D-QSARs. *Current drug discovery technologies*, 2, 13-21.
- RAO, Y. S., PRASAD, M., SRI, N. U. & VEERAIHAH, V. 2016. Vibrational (FT-IR, FT-Raman) and UV–Visible spectroscopic studies, HOMO–LUMO, NBO, NLO and MEP analysis of Benzyl (imino (1H-pyrazol-1-yl) methyl) carbamate using DFT calculations. *Journal of Molecular Structure*, 1108, 567-582.
- ROCHA, M., DI SANTO, A., ARIAS, J. M., GIL, D. M. & ALTABEF, A. B. 2015. Ab-initio and DFT calculations on molecular structure, NBO, HOMO–LUMO study and a new vibrational analysis of 4-(dimethylamino) benzaldehyde. *Spectrochimica Acta Part A: Molecular and Biomolecular Spectroscopy*, 136, 635-643.
- SCROCCO, E. & TOMASI, J. 1978. Electronic molecular structure, reactivity and intermolecular forces: an euristic interpretation by means of electrostatic molecular potentials. *Advances in quantum chemistry*. Elsevier.
- SHANKAR, R., SENTHILKUMAR, K. & KOLANDAIVEL, P. 2009. Calculation of ionization potential and chemical hardness: a comparative study of different methods. *International Journal of Quantum Chemistry*, 109, 764-771.
- WARE, E. 1950. The chemistry of the hydantoins. *Chemical Reviews*, 46, 403-470.